# Buck Power Supply for Racing Motorcycles Electronic Systems

E. Borsetto*, S. Buso**, G. Spiazzi**

* aprilia racing

Via Galileo Galilei 1 - 30033 - Noale (VE) - ITALY
Phone:+39.041.582.9111 Fax:+39.041.582.9750
E-Mail: borsetto_emanuele@aprilia.it

**Department of Electronics and Informatics - University of Padova
Via Gradenigo 6/a - 35131 Padova - ITALY
Phone:+39.49.827.7503/7517 Fax:+39.49.827.7599/7699
E-Mail: simone@tania.dei.unipd.it

**Abstract - The design and practical implementation of a Buck power supply for racing motorcycles is described. The converter is used to interface the motorbike rotating generator with the battery in order to maintain its charge and increase the quality of the dc supply voltage for the different electronic systems on board. The need for minimum size and weight together with the capability of generating an output power of about 200 W are the basic design constraints. The paper describes the adopted design procedure and presents the results of the experimental tests that have been performed to check the validity of the design. In particular, the typical large signal features of the converter such as the start-up, overload and short circuit modes of operation are illustrated, together with small signal characteristics, including audiosusceptibility and output voltage regulation in the presence of load variations.**

## I. Introduction

Racing motorcycles require a large amount of electronic systems on board, both for the optimization of the mechanical systems' performance and for diagnostic and control functions. The availability of a reliable power supply is therefore vital for the successful operation of the motorbike during tests and competitions. As far as the power range is concerned, the typical peak supply power can be estimated in about 200 W. While the use of spendable batteries is certainly a viable solution, the supply of the motorbike electronic systems by means of a rotating generator coupled with a voltage regulator is the strategic choice motivating the project this paper deals with. When it comes to this kind of applications of power electronics, the main design constraints are of course the minimization of the final size and weight of the converter, but also its ruggedness and reliability, which are indeed vital characteristics, given the typical extremely hard environmental conditions it has to sustain. Another relevant aspect is the achievement of a good efficiency; being the dissipation capability of the final packaged converter quite limited, a reasonable operating temperature in the worst case conditions must be guaranteed by minimizing the losses. Of course, the capability of the converter to tolerate output short-circuits and other typical fault conditions implying significant overloads is also important. As far as the dynamic performance is concerned, the converter must be optimized especially under the audiosusceptibility point of view, in order to allow the reduction of the capacitive filter in the rectifier unit, which is directly connected to the rotating generator. Another fundamental aspect is the minimization of the circuit susceptibility to conducted EMI, which is typical in the automotive environment and even more critical in a racing motorbike. This implies the adoption of suitable design provisions in the PCB implementation. The paper illustrates all of these topics, discussing the adopted design criteria and providing experimental verification of the achieved final design.

## II. Power Converter Design

The design specifications for the power converter can be summarized as follows. The input voltage of the converter is the rectified and filtered output voltage of a rotating synchronous generator. The output characteristic of the rotating generator, directly connected to the typically adopted 12 V battery, is plotted in Fig. 1. As can be seen, the current capability of the generator is quite high, and therefore a similar current capability must be guaranteed also by the converter interfacing it to the battery. As a matter of fact, the expected load for the converter is given by the following:

$$I_{Load}[mA] = 6000 + 0.5 \cdot RPM \,, \qquad (1)$$

which sets the maximum load current (corresponding to

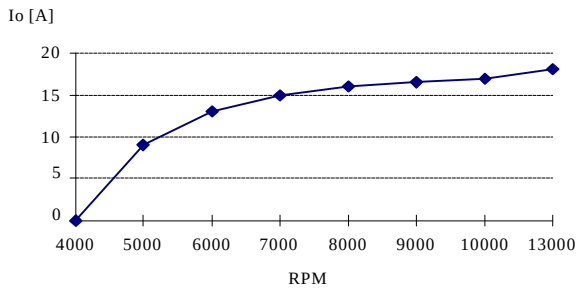


Fig. 1 - Synchronous generator output characteristic: generated output current as a function of RPM. The generator is connected to the 12 V battery.

about 20,000 RPM) to 16 A. Therefore, this is the nominal output current the battery charger is designed for. As far as the input voltage is concerned, this depends on the type of synchronous generator which is installed on the bike. To be able to interface the battery charger with all the types of available generators a worst-case maximum input voltage of 75 V is taken into account. The specifications are summed-up in Table I.

TABLE I
BATTERY CHARGER SPECIFICATIONS

| | |
|---|---|
| Minimum Input Voltage | 20 V |
| Maximum Input Voltage | 75 V |
| Output Voltage | 13.5 V |
| Output Voltage Static Precision | 0.1 V |
| Output Voltage Peak Ripple | 1 V |
| Minimum Load Current | 6 A |
| Nominal Output Power | 220 W |

Given these specifications, the buck converter appears to be a good topology, capable of achieving the desired performance with reduced complexity and therefore high ruggedness and reliability, combined also with minimum size and weight. In Fig. 2, a schematic of the adopted topology and control strategy is shown. As can be seen, the adopted scheme allows to drive the power switch without insulation, which greatly reduces the circuit complexity. The main disadvantage of such a solution is, of course, the floating output voltage feedback signal. The fundamental points of the converter design can be identified in the selection of the power switch and diode, in the design of the inductor and the choice of input and output capacitors. These are discussed in the following.

*A. Selection of the power switch and diode.*

The switch must exhibit minimum $R_{DSon}$, so as to minimize conduction losses; the switching losses have to be minimized by achieving fast turn on and turn off times (< 50 ns) suitably designing the driving circuitry. The inclusion of snubber circuits has to be avoided to minimize the losses and the final converter's volume. The diode solution must be compared to synchronous rectification: an accurate estimation of the losses on the active devices, based on numerical simulations taking into account the different possible operating conditions of the converter, demonstrates that, in this application, the use of Schottky diodes is globally advantageous with respect to synchronous rectification. As a consequence, a couple of parallel connected Schottky diodes has been used in this design.

*B. Design of the filter inductor*

The inductor must be of the smallest size compatible with a sufficient inductance value to achieve current ripple reduction. The design procedure involves the calculation of the needed inductor value from the desired ripple, given the desired switching frequency and taking into account the variability of the input voltage and of the load current (which are not independent from each other). After that, the expected core thermal stress for different core sizes and materials has to be computed. This calculation has been based on the models provided by the core manufacturer and, therefore, can only be considered a first order approximation. According to those models, to reduce the thermal stress, either the inductor value or the switching frequency can be increased. The former choice is constrained by the limit in the core size, the latter is constrained by the switching losses. An optimum solution can be found, essentially by trials and errors, which trades off these two factors. In our final design, the converter adopts the 77310-A7 Kool-Mμ€® core, where 15 turns of AWG 10 copper wire are wound, corresponding to an inductance of about 10 μH. The final value for the switching frequency is set slightly higher than 250 kHz.

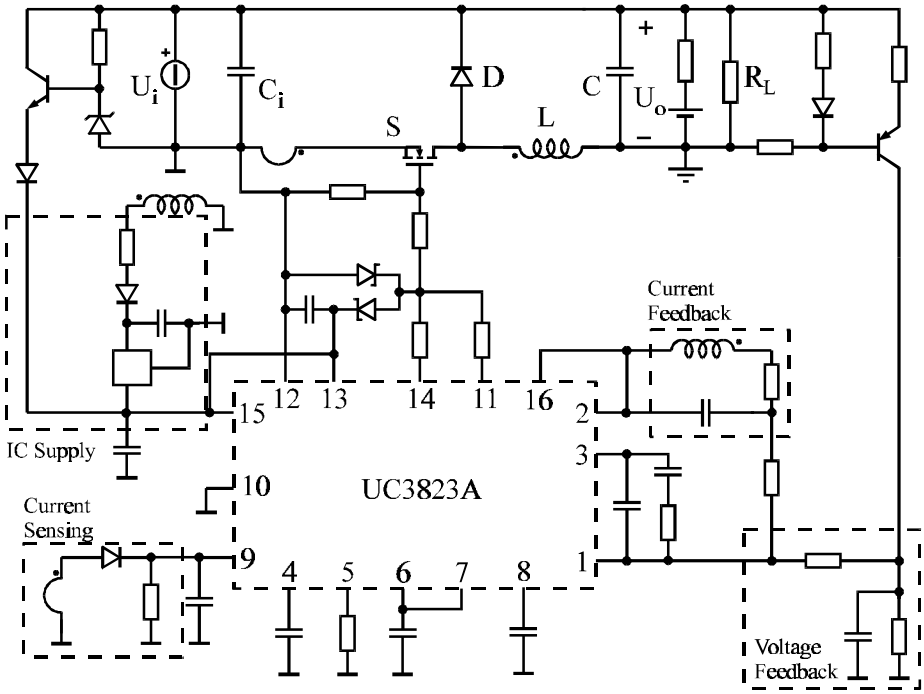


Fig. 2 - Simplified schematic of the converter and control IC

*C. Design of the filter capacitors*

High quality, low ESL, low ESR, high operating temperature capacitors have to be used in this design for two basic reasons: the converter has to produce a very low ripple on the battery and is required to operate in a very hot environment. Indeed, despite the apparent efficient cooling, the chassis of the motorbike, where the converter is located, can get to temperatures as high as 65 °C, which can be steadily maintained for long periods during the race. As far as the output capacitors are concerned, these have to drain the high frequency current ripple generated by the converter and prevent this to affect the battery. Similar features are required also to the input capacitors, since these have to cope with the rectified voltage ripple, which in this application can be quite high in frequency (about 2 kHz). From this standpoint, the audiosusceptibility of the converter is a key factor, since its reduction allows to reduce the input capacitance required to limit the induced ripple on the output voltage. Therefore, in the choice of the control strategy this has been considered a fundamental constraint.

The final values for the main components of the power converter are summed-up in Table II.

TABLE II
CONVERTER MAIN COMPONENTS

| | | |
|---|---|---|
| Mosfet (S) | IRFP150 | 40A, 100V |
| Diode (D) | 30CPQ100 | 30A, 100V |
| Inductor (L) | 10μH | 15 turns, Kool-Mμ® core |
| Input Capacitor ($C_i$) | 220μF + 2.2μF | Low ESR, low ESL |
| Output Capacitor (C) | 47μF+2.2μF | Low ESR, low ESL |

## III. CONTROL STRATEGY

Initially, voltage mode control was chosen as the converter's control strategy. This had the advantage of minimizing the control's complexity, while fulfilling the given specifications. However, after some preliminary tests, the converter audiosusceptibility turned out to be too high, especially in the high frequency range (between 1 and 2 kHz), where the input voltage ripple frequency lies. To improve this parameter, so as to allow the reduction of the input filter capacitance, an additional current loop has been added to the control. Its implementation has been done by means of a suitably designed integrator on the inductor voltage, rather than using the current sensor included in the converter's hardware, which is used only for protection purpose. As far as the dynamic and small signal properties of the control are concerned, this solution offers a good performance level, comparable with the usual current feedback implementation. Moreover, being the current feedback signal reconstructed by means of analog integration, this solution strongly reduces the susceptibility of the current control to disturbances and noise, allowing the design to be less conservative. As a result of the adoption of this control strategy, the audiosusceptibility of the converter has been reduced in

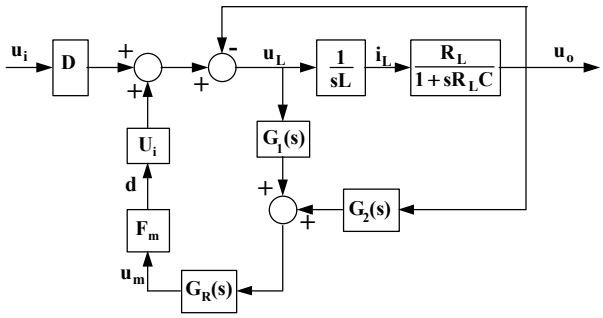


Fig. 3 - Control block diagram with the different involved transfer functions: $G_R(s)$ = PI regulator; $F_m$ = modulator gain; $G_1(s)$ = inductor voltage integrator; $G_2(s)$ = output voltage transducer; D = steady state duty-cycle.

the range of interest of about 20 dB. The theoretical basis for this control technique has been found in [1]. The equivalent block diagram of the implemented controller, together with the model of the power stage, is shown in Fig. 3. To design the control parameters, small signal analysis on an averaged converter model has been employed. The Bode plot of the system open loop gain $G_{ol}(s)$ is shown in Fig. 4, both for minimum and maximum input voltage. As can be seen, because of the fairly high variation of the loop gain, the crossover frequency may go from 9.2 to 25 kHz.

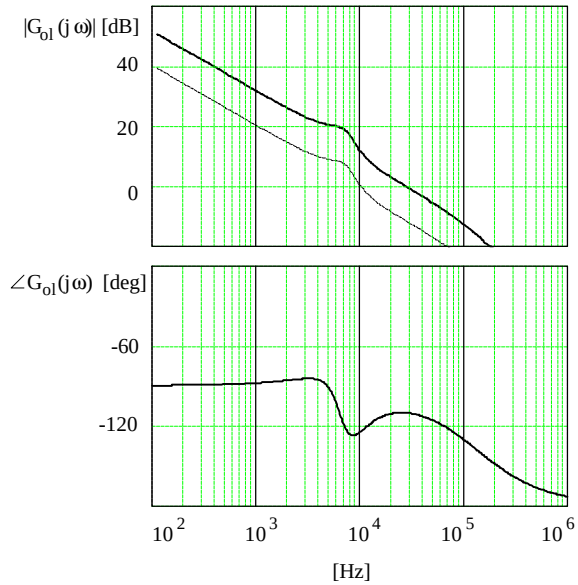


Fig. 4 - Bode plot of system open loop gain $G_{ol}(j\omega)$: solid line refers to maximum $U_i$, dashed line to minimum $U_i$.

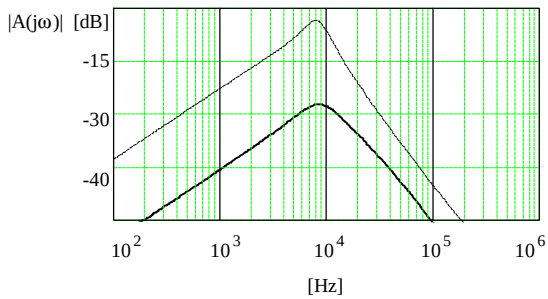


Fig. 5 - Bode plot of system audiosusceptibility $A(j\omega)$: solid line refers to maximum $U_i$, dashed line to minimum $U_i$.

Fig. 5, instead, shows the system's expected audiosusceptibility, again for minimum and maximum input voltage. Given the control's bandwidth variation with the input voltage, the maximum rejection of disturbances injected at the converter's input takes place when the input voltage is maximum.

## IV. PCB DESIGN

As already stated, the minimization of the size of the converter necessary for this kind of application poses the problem of the coexistence in a very small volume of power and control circuitry. It is therefore of paramount importance that the design of the printed circuit board is carefully performed in order to minimize the typical noise and disturbance problems which may occur. In order to do that, some practical design rules have been applied, which can also be partially found in [2]. It is worth noting that the main issue here is the auto-compatibility of the circuit. In fact, since the converter is going to be closed inside an high quality metallic box with all the necessary passing EMI filters on the cables and so on, no EMI problems are expected to come from the external environment or to be generated outside the box. Therefore only auto-compatibility is expected to be an issue. The key points are the routing and shielding of the high dv/dt tracks and the minimization of the areas embraced by the high di/dt tracks, which are, of course, equivalent to loop antennas. The use of cold tracks as shields for the hot ones together with the adoption of separate ground planes for the power and signal circuits are some of the typically adopted

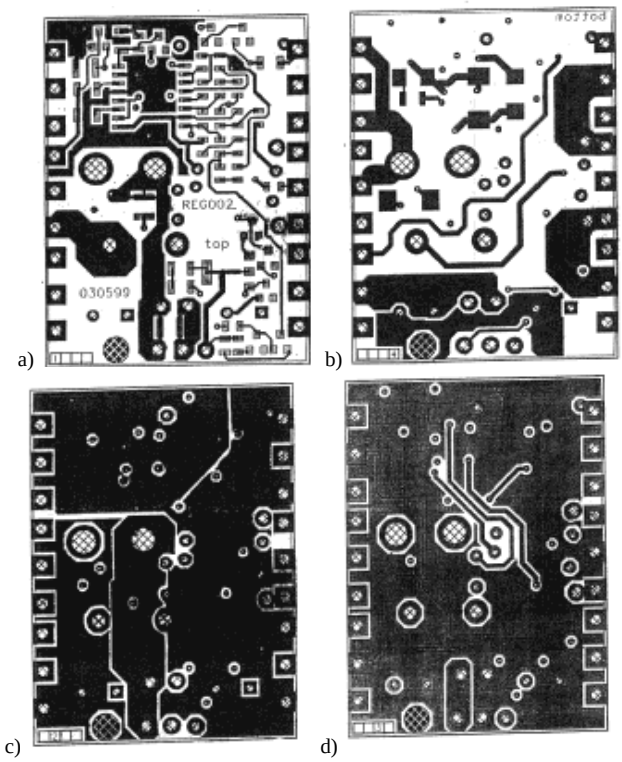


Fig. 6 - The four layers of the PCB: a) top (control) layer; b) bottom (power) layer; c) internal layer connected to positive supply; d) internal layer connected to ground.

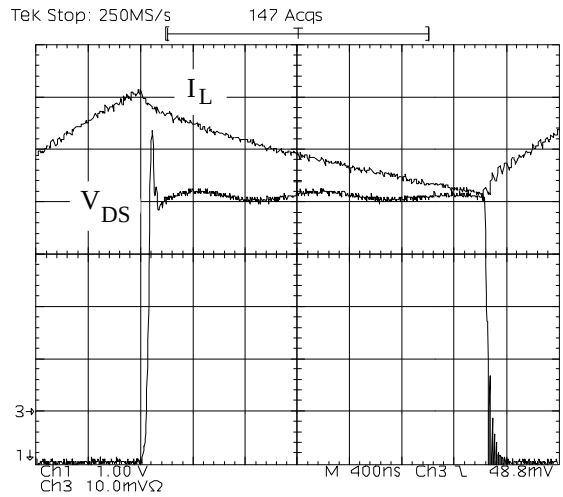


Fig. 7 - Mosfet drain-source voltage $V_{DS}$ (10 V/div; 400 ns/div) and converter current $I_L$ (2 A/div; 400 ns/div) @ $I_o$=10 A

solutions. In this particular case, the power components are placed on the top layer of the adopted 1.6 mm thick, four layer board, while the power components are placed on the bottom one, being the internal layers almost fully occupied by metal planes connected to the supply and ground voltage. These are used as electric shields, so as to protect the control circuit from the EMI generated by the power circuit. The bottom and top layers of the PCB are shown in the upper part of Fig. 6. It is possible to see how the ground track is extended around the control IC pins (Fig. 6.a, top, left) so as to create a local ground plane. This is designed to closely surround the sensitive tracks, i.e. feedback tracks, to improve their immunity to noise. The critical paths, e.g. the gate track, are all kept very short, to minimize the stray inductance. High quality capacitors are used to close the high di/dt loops so as to minimize the radiating area in the power components layer. The internal layers are shown in the lower part of Fig. 6.

## V. EXPERIMENTAL TESTS

A lot of experimental tests have been performed on the designed converter to verify the expected performance. The converter data, referring to a full load operating condition, are reported in Table III. The measured

TABLE III
CONVERTER TEST AT FULL LOAD

| | |
|---|---|
| Input voltage | $U_i$ = 59V |
| Input Current | $I_i$ = 4.3A |
| Input Power | $P_i$ = 253.7W |
| Output Voltage | $U_o$ = 13.24 |
| Output Current | $I_o$ = 16.6A |
| Output Power | $P_o$ = 220W |
| Switching Frequency | $f_{sw}$ = 260 kHz |
| Estimated Efficiency | $\eta$ = 86.6% |

inductor current is shown in Fig. 7, together with the behavior of the drain-source voltage of the Mosfet. It is worth noting that this is a snubberless solution; this is necessary to minimize the turn-on and turn-off times of the switch and consequently increase the converter

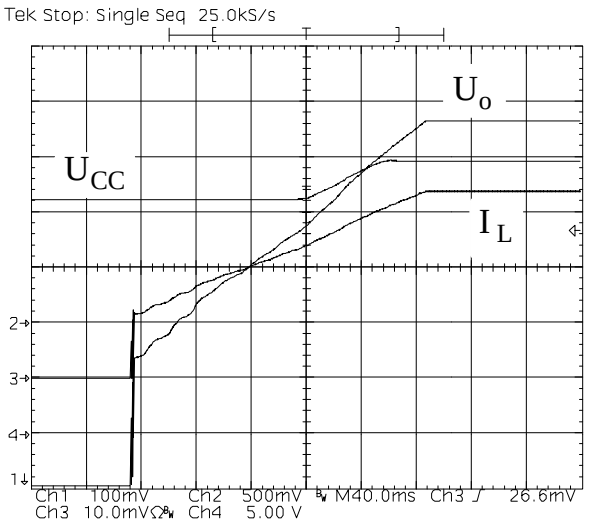


Fig. 8 - Converter start-up @ $I_o$ = 16.6A. Pin 8 voltage $U_{CC}$ (5 V/div, 40 ms/div), inductor current $I_L$ (5 A/div, 40 ms/div), output voltage $U_o$ (2 V/div, 40 ms/div).

efficiency. As a consequence, the overshoot on the drain voltage can be controlled only by carefully designing the circuit layout.

The converter behavior at the start-up is shown in Fig. 8. As can be seen, a linearly increasing output voltage and current are achieved, reaching the steady-state level after about 200 ms, duration arbitrarily chosen and subject to variations in the final implementation. The converter initially gets the supply from the input and starts commutating at the minimum operating voltage, which is about 20 V. When the output voltage is high enough the converter gets the supply through an auxiliary winding and a linear regulator, while the input circuit goes off.

The converter's behavior in the presence of load step variations is shown in Fig. 9 and Fig. 10. Both are obtained with the battery connected at the output which explains the duration of the transient and the reduced output voltage variation (2.7 V). It is worth remarking that the output capacitance internally included in the converter is less than 50 μF.

Fig. 11 shows the converter's behavior in the presence of a short-circuit at the output. As can be seen, when the output voltage drops to zero, the converter's current tends to rapidly increase but, as soon as it reaches the overcurrent protection limit, which is set to about 23 A, corresponding to a 50% overload capability, it is clamped. Actually, the clamping is very short because, being the controller supplied from the output, immediately after the short circuit takes place, the control shuts down. Therefore, also the input current goes to zero. This condition implies the occurrence of several start-up cycles, as the one showed in the figure. Of course, none of them is able to turn the system on, until the short-circuit condition is removed.

The audiosusceptibility of the converter is illustrated by Fig. 12, where the input voltage and the corresponding output voltage are shown. The converter in this case has been connected to the rotating generator on board the

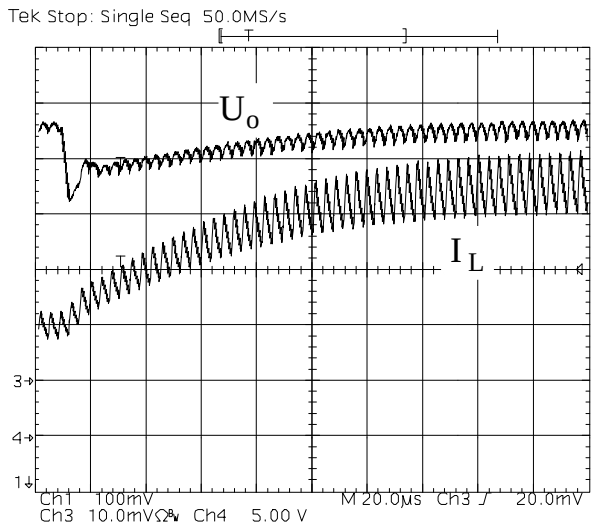


Fig. 9 - Load step change with battery connected at the output: $\Delta I_L$ = 12.7 A, $\Delta U_{oMAX}$ = -2.7 V. Inductor current $I_L$ (5 A/div, 20 μs/div), output voltage $U_o$ (2 V/div, 20 μs/div).

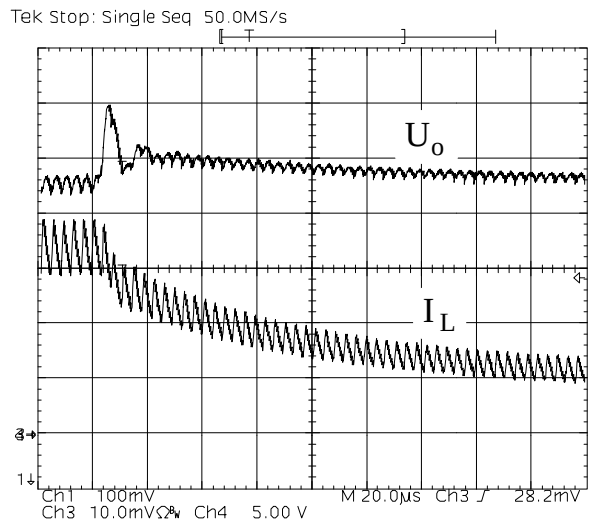


Fig. 10 -Load step change with battery connected at the output: $\Delta I_L$ = -12.7 A, $\Delta U_{oMAX}$ = +2.7 V. Inductor current $I_L$ (5 A/div, 20 μs/div), output voltage $U_o$ (2 V/div, 20 μs/div).

motorbike. The generator has been brought to about 11,000 RPM, so that it could produce an input voltage of about 55 V (average value), with a superimposed ripple of about 9 V (peak to peak) having a frequency of about 1.3 kHz. The converter load was set to 15 A, close to the nominal value, and the output voltage on the 12 V battery was measured. As can be seen, the controller is able to guarantee a considerable rejection of the input voltage ripple, allowing to satisfy the design specification with a little output capacitance. The measured output voltage is affected by a ripple of about 110 mV (peak to peak), which implies a -38 dB attenuation. As can be seen, this is in good agreement with the theoretical forecast of Fig. 5. Other similar measurements were performed in different operating conditions, all confirming the expected converter's behavior.

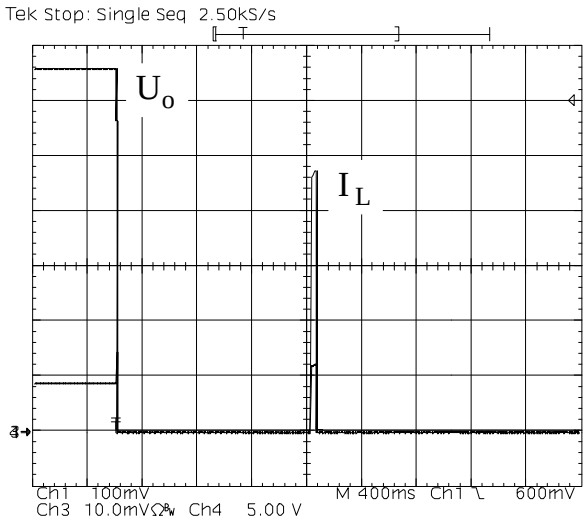


Fig. 11 - Short circuit operation. Inductor current $I_L$ (5 A/div, 400 ms/div), output voltage $U_o$ (2 V/div, 400 ms/div). Note the overcurrent protection limit set to about 23 A (50% overload).

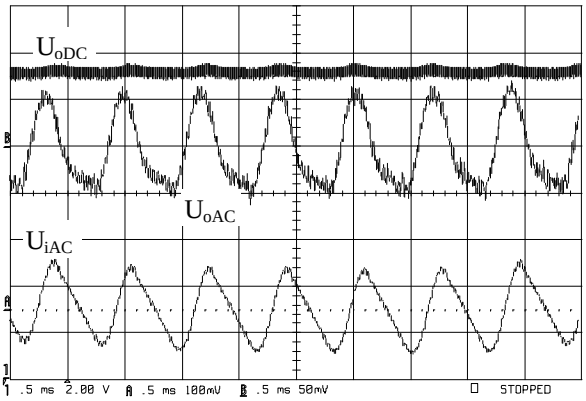


Fig. 12 - Input voltage ripple rejection. DC coupled output voltage $U_{oDC}$ (2 V/div, 500 µs/div), AC coupled output voltage $U_{oAC}$ (50 mV/div, 500 µs/div), AC coupled input voltage $U_{iAC}$ (5 V/div, 500 µs/div).

To give an idea of the final result of this design, Fig. 13 shows a picture of the converter in its package. The picture is taken from the bottom, with the bottom of the package removed. As can be seen the final volume of the aluminum package is quite small (length: 85 mm, width: 56 mm, depth: 28 mm) and so is the weight (270 g including the resinous filler). The total volume of the packaged converter (including also the heatsink's volume) is about 133 $cm^3$, determining a power density of about 1.6 $W/cm^3$ ($\cong$ 27 $W/in^3$). Fig. 14 finally shows the converter installed on the Aprilia RSW500, which races in the 1999 world championship in the 500 class.

## VI. Conclusions

The design and implementation of a Buck converter to be used as a power supply for racing motorcycles is described. The converter is used as an interface between a diode bridge rectifier connected to the motorbike rotating generator and the battery. Its basic function is to maintain the battery charge and to increase the quality of the dc voltage supplied to the different electronic systems present

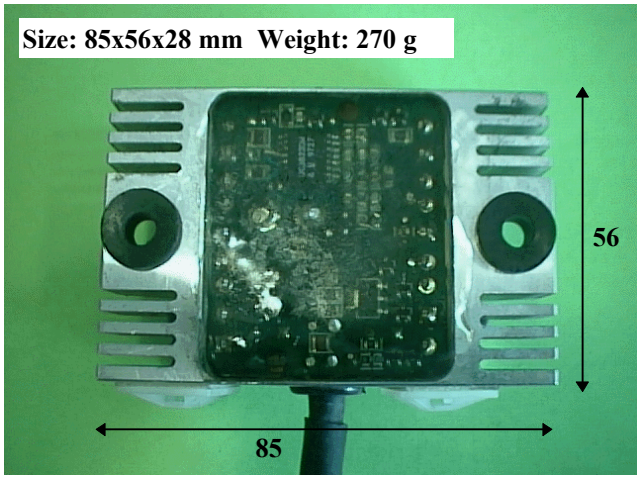


Fig. 13 - Final converter with size and weight

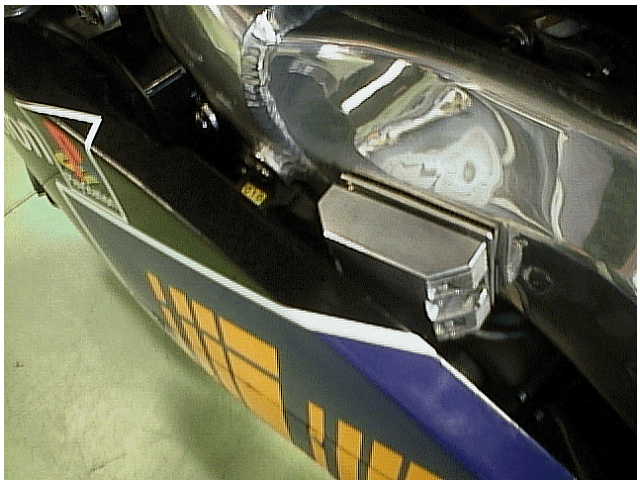

Fig. 14 - Final converter on the motorbike.

on board the motorbike. The need for minimum size and weight together with the capability of generating a peak output power of about 200 W are the basic design constraints. The paper describes the adopted design procedure and motivates the basic design choices. It finally presents some of the results of the experimental tests that have been performed to check the validity of the design.

## VII. References

[1] P. Midya, M. Greuel, P.T. Krein, "Sensorless Current Mode Control - An Observer-Based Technique for DC-DC Converters", IEEE Power Electronics Specialist Conference, St. Louis, 1997, pp. 197-202.

[2] Power Integrations, Inc., Power Integrated Data Book, Design Aid DA-2, "Circuit Board Layout with the PWR-SMP Family", 1991, pp. 4-49, 4-58.